RSC Advances

This article can be cited before page numbers have been issued, to do this please use: X. Chen, S. Shan, J. Liu, X. Qu and Q. Zhang, *RSC Adv.*, 2015, DOI: 10.1039/C5RA15321B.

ROYAL SOCIETY OF CHEMISTRY

www.rsc.org/advances

View Article Online
DOI: 10.1039/C5RA15321B

Journal Name

ARTICLE

Synthesis and properties of high temperature phthalonitrile polymers based on o, m, p-dihydroxybenzene isomers

Received 00th January 20xx,
Accepted 00th January 20xx

DOI: 10.1039/x0xx00000x

www.rsc.org/

Xinggang Chen[a,b,c], Shuyan Shan[b], Jiayu Liu[b], Xiongwei Qu,[a,b] Qingxin Zhang[a,b*]

A series of high-temperature phthalonitrile monomers with o, m, p-dihydroxybenzene isomers, namely, 1,2-bis(3,4-dicyanophenoxy) benzene (o-BDB), 1,3-bis(3,4-dicyanophenoxy) benzene (m-BDB) and 1,4-bis(3,4-dicyanophenoxy) benzene (p-BDB), were synthesized via a facile nucleophilic displacement of a nitro-substituent from 4-nitrophthalonitrile. The structures of the monomers were characterized by FTIR, 1H NMR and WXRD. Curing behaviors of the monomers with 4,4¢-diaminodiphenyl ether were recorded by DSC. The result shows that the processabilities of o-BDB and m-BDB are superior to p-BDB due to lower melting points and broader processing windows. The structures of the cured phthalonitrile polymers were characterized by FTIR and WXRD, and thermal stabilities were evaluated by TGA and all the polymers exhibit excellent thermal and thermal-oxidative stabilities. Dynamic mechanical analysis reveals that the polymers have high storage modulus and high glass-transition temperatures. Consequently, o-BDB and m-BDB polymers show more outstanding processability, thermal stability and mechanical property than p-BDB polymers, which may be good candidates of high-temperature phthalonitrile polymers.

Introduction

Phthalonitrile polymers are a versatile class of high-temperature resins and have drawn great attention for their exceptional properties, such as outstanding thermal and thermo-oxidative stability, excellent mechanical properties and superior fire resistance. Those attractive properties make these polymers potential candidates for advanced composite matrices, adhesives, microelectronic packing materials, etc.[1,2] Previous studies on phthalonitrile polymers have concentrated on novel bifunctional phthalonitrile monomers, self-catalyzed functional phthalonitrile monomers[3-7] and phthalonitrile composites[8-13]. Main properties of bifunctional phthalonitrile monomers contain melting temperature, curing temperature, processing windows - defined as the temperature between melting temperature and curing temperature, and curing density, which are influenced by a variety of monomer structures.

In general, the introduction of flexible aromatic ether linkages into the monomer structure tends to result in decreasing melting temperature and then increasing processing windows. Various bifunctional phthalonitrile monomers containing alkyne[14], benzoxazine[15,16], aromatic ether nitrile[17], alkyl-center-trisphenols[18], aromatic ether[19], novolac[20,21], imide[4], bisphenol-A[22,23], naphthyl[24], biphenyl ethernitrile[25,26], heterocycle[27], sulfone linkages[28,29] between terminal phthalonitrile units have been reported. However, these flexible aromatic ether linkages also compromise thermal stability and mechanical properties of phthalonitrile polymers. Moreover, the more flexible aromatic ether linkages in the monomer are, the greater performance losses of phthalonitrile polymers are. At the same time, complex aromatic ether linkages are adverse to the synthesis and purification of novel monomers and the processability of phthalonitrile polymers. Therefore, it is desirable to modify the structure of phthalonitrile monomers to choose simple, familiar, economical and effective aromatic ethers. M-dihydroxybenzene has been preciously introduced into phthalonitrile monomers, which has resulted in phthalonitrile polymers with outstanding thermal properties.[19]

In this report, a series of phthalonitrile monomers based on o, m, p-dihydroxybenzene isomers, *viz*. 1,2-bis(3,4-dicyanophenoxy) benzene (o-BDB), 1,3-bis(3,4-dicyanophenoxy) benzene (m-BDB) and 1,4-bis(3,4-dicyanophenoxy) benzene (p-BDB), were synthesized. The structures of the phthalonitrile monomers and polymers were characterized by Fourier transform infrared spectroscopy (FTIR), nuclear magnetic resonance spectroscopy (^{1}H NMR) and wide-angle X-ray diffraction (WAXD). Curing behaviors of three monomers were recorded by differential scanning calorimetric (DSC). Thermal stability and dynamic mechanical properties of phthalonitrile polymers were evaluated and compared by thermogravimetric analysis (TGA) and dynamic mechanical analysis (DMA).

[a] *Key Lab for Micro- and Nano-Scale Boron Nitride Materials in Hebei Province, School of Materials Science and Engineering, Hebei University of Technology, Tianjin 300130, China.*
[b] *Institute of Polymer Science and Engineering, School of Chemical Engineering and Technology, Hebei University of Technology, Tianjin 300130, China. E-mail: zhqxcn@163.com*
[c] *Hebei Province Key Laboratory of Inorganic Nonmetallic Materials, School of Materials Science and Engineering, North China University of Science and Technology, Tangshan, Hebei 063009, China*
Electronic Supplementary Information (ESI) available: Experimental details ofNMR and FTIR spectra, XRD crystallographic data. See DOI: 10.1039/x0xx00000x

View Article Online
DOI: 10.1039/C5RA15321B

Experimental

Materials

O-dihydroxybenzene (o-DB, AR, > 99.0 %), m-dihydroxybenzene (m-DB, AR, > 99.0 %) and p-dihydroxybenzene (p-DB, AR, > 99.0 %) were purchased from Alfa Aesar. 4-nitrophthalonitrile (NPN, AR, > 98.0 %) was purchased from Wuhan Chifei Chemical Corporation, China. 4,4′-Diaminodiphenyl ether (ODA, AR, > 98.0 %) was obtained from Beijing Hengye Zhongyuan Chemical Corporation. Potassium carbonate (K_2CO_3, AR, > 99.0 %) was purchased from Tianjin Fengchuan Chemical Corporation. The above chemicals were dried over night at 85 °C under vacuum before use. All the solvents were used without further purification.

Synthesis

Synthesis of o-BDB, m-BDB and p-BDB monomers. To a 250 mL, three-necked flask was added o-dihydroxybenzene (2.02 g, 18.34 mmol), pulverized anhydrous potassium carbonate (6.34 g, 47.98 mmol), and dry DMF (50 mL). The mixture was heated to 90 °C with stirring and held at this temperature for 0.5 h. The reaction mixture changed from colorless to reddish brown gradually. Then 4-nitrophthalonitrile (6.35 g, 36.70 mmol) was added in one portion and the resulting mixture was kept at this condition for 8 h under a nitrogen atmosphere. Finally, after the reddish brown product mixture was cooled to ambient temperature, 300 mL deionized water was poured into it. The product was repeatedly washed by suction filtration with plenty of deionized water until the filtrate was pellucid. The filtered 1,2-bis(3,4-dicyanophenoxy) benzene (o-BDB) product was dried overnight under vacuum at 60 °C. Yield: 92 %. Melting point (T_m): 183.5 °C (determined by DSC). ^{1}H NMR (400 MHz, DMSO-d_6, δ): 8.04 (d, *J* = 8.53 Hz, 2H, ArH-2), 7.76 (d, *J* = 2.51 Hz, 2H, ArH-1), 7.46 (d, *J* = 2.51 Hz, 2H, ArH-3), 7.38 (d, *J* = 2.51 Hz, 2H, ArH-4), 7.36 (d, *J* = 2.51 Hz, 2H, ArH-5). FTIR (KBr, cm^{-1}): 3076 and 845 (ArC-H), 2233 (-CN), 1598 (ArC=C), 1246 (C-O-C).

1,3-bis(3,4-dicyanophenoxy) benzene (m-BDB) and 1,4-bis(3,4-dicyanophenoxy) benzene (p-BDB) were synthesized in the same procedures as 1,2-bis(3,4-dicyanophenoxy) benzene (o-BDB) by replacing o-dihydroxybenzene (o-DB) with m-dihydroxybenzene (m-DB) and p-dihydroxybenzene (p-DB), respectively.

For 1,3-bis(3,4-dicyanophenoxy) benzene (m-BDB), Yield: 90 %. Melting point (T_m): 183.6 °C (determined by DSC). ^{1}H NMR (400 MHz, DMSO-d_6, δ): 8.13 (d, *J* = 8.78 Hz, 2H, ArH-2), 7.92 (d, *J* = 2.51 Hz, 2H, ArH-1), 7.60 (t, *J* = 8.28 Hz, 2H, ArH-3), 7.55 (d, *J* = 8.78 Hz, 2H, ArH-6), 7.15 (s, 2H, ArH-5), 7.13 (s, 2H, ArH-4). FTIR (KBr, cm^{-1}): 3077.8 and 851.9 (ArC-H), 2233.2 (-CN), 1598.4 (ArC=C), 1251.6 (C-O-C).

For 1,4-bis(3,4-dicyanophenoxy) benzene (p-BDB), Yield: 91 %. Melting point (T_m): 251.5 °C (determined by DSC). ^{1}H NMR (400 MHz, DMSO-d_6, δ): 8.15 (d, *J* = 8.78 Hz, 2H, ArH-1), 7.88 (d, *J* = 2.51 Hz, 2H, ArH-2), 7.52 (d, *J* = 8.78 Hz, 2H, ArH-3), 7.34 (s, 2H, ArH-4). FTIR (KBr, cm^{-1}): 3072 and 841 (ArC-H), 2233 (-CN), 1598 (ArC=C), 1248 (C-O-C).

Preparation of o-BDB, m-BDB and p-BDB prepolymers and polymers. O-BDB, m-BDB and p-BDB polymers were prepared through a two-step method in presence of ODA as curing additive. The first step was that ODA (0.097 g, 0.485 mmol) was added into the monomer (10.0 g, 0.024 mol) and stirred homogeneously, then moved into a mold and melted under vacuum at 150 °C for 20~30 min until the viscosity of the molten system without bubbles increased. The second step was to prepare o-BDB, m-BDB and p-BDB polymers in a muffle furnace and then postcure at elevated temperatures by a heating protocol: 220 °C / 2 h, 260 °C / 4 h, 300 °C / 4 h, 340 °C / 4 h, 380 °C / 6 h.

Characterization methods

^{1}H NMR spectra of o-BDB, m-BDB and p-BDB monomers were obtained by a Bruker 400 MHz nuclear magnetic resonance (NMR) spectrometer with DMSO-d_6 as solvent. Fourier Transform Infrared (FTIR) spectra of o-BDB, m-BDB and p-BDB monomers and polymers were recorded on a Bruker Vector 22 FTIR spectrophotometer in KBr pellets between 4000 and 400 cm^{-1}. Wide-angle X-ray diffraction (WAXD) was conducted with a Bruker lynxeye detector (D8 FOCUS) operating at 40 kV and 40 mA with Ni-filtered Cu Kα radiation (λ = 0.15406 nm) in reflection mode. The 2θ was collected from 2 to 60 ° with interval of 0.02 ° at a scanning speed of 4 ° min^{-1}. Differential scanning calorimetric (DSC) study was performed on a PE Diamond DSC from 50 to 400 °C at a heating rate of 10 °C min^{-1} with a nitrogen flow rate of 100 mL min^{-1}. Thermogravimetric analysis (TGA) was performed using a TA Instruments Q600 thermogravimetric analyzer at a heating rate of 10 °C min^{-1} under nitrogen and air atmosphere with a flow rate of 100 mL min^{-1}, respectively. DMA was performed on a DMA Q800 (TA Instruments) in dual cantilever mode with a driving frequency of 1 Hz, an amplitude of 10 μm and a heating rate of 10 °C min^{-1} in nitrogen atmosphere.

Results and discussion

Synthesis

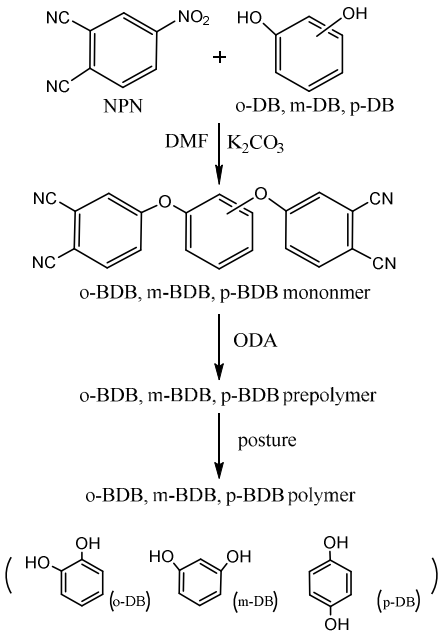

Fig. 1 Synthesis and polymerization of o-BDB, m-BDB and p-BDB monomers, prepolymers, and polymers

O-BDB, m-BDB and p-BDB monomers were synthesized by a nucleophilic displacement of a labile nitro-substituent from NPN with three isomers of dihydroxybenzene (o-DB, m-DB, p-DB) using

View Article Online
DOI: 10.1039/C5RA15321B

DMF as a solvent according to the reaction sequence as depicted in Fig. 1.

FTIR and ^{1}H NMR techniques were employed to characterize the structures of o-BDB, m-BDB and p-BDB monomers. As mentioned in the experimental section, all the FTIR and ^{1}H NMR peaks assigned were in complete agreement with the proposed molecular structures (Fig I, II, III and IV in Supplementary Information). FTIR spectra of o-BDB, m-BDB and p-BDB monomers show that the absorption peaks at 3099 and 700~900 cm^{-1} are corresponding to aromatic C-H stretching vibration and aromatic C-H bending vibration, respectively. It is noticed that a strong absorption peak centered at 2235 cm^{-1} appears, which is the characteristic stretching of nitrile group (-C≡N). The absorption bands within 1411~1587 cm^{-1} should be ascribed to the stretching of phenyl rings, and the peak at 1250 cm^{-1} is due to C-O-C stretching. The results of FTIR and ^{1}H NMR show that three monomers with target structures are obtained.

XRD patterns of o-BDB, m-BDB and p-BDB monomers are shown in Fig. 2. Miller indices, namely, (h k l), were calculated by Jade analysis software through a set of possible XRD reflections using the initial cell, and the miller indices are marked in Fig. 2 (Table I, II and III in Supplementary Information). The cell parameters of the monomers are determined by a trial and error method, and the result is further refined by a least-square procedure. The experimental and calculated cell parameters are listed in Table 1. Three unit cells are determined to be monoclinic with a volume of 1316.65 Å^3, triclinic with a volume of 918.29 Å^3 and monoclinic with a volume of 1831.93 Å^3, respectively, where the differences of cell types and cell volumes should be ascribed to their molecular structures.

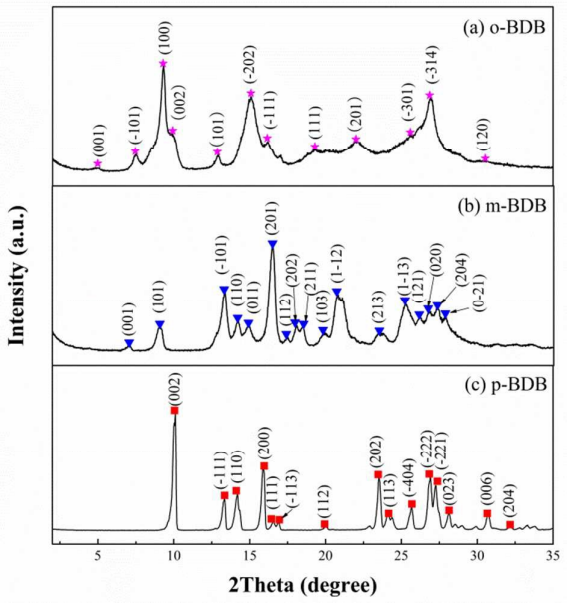

Fig. 2 XRD patterns of (a) o-BDB, (b) m-BDB and (c) p-BDB monomers

Table 1 Cell parameters of o-BDB, m-BDB and p-BDB monomers

Cell parameters	o-BDB monomer			m-BDB monomer			p-BDB monomer		
	Initial Cell	Refined Cell	Δ/%	Initial Cell	Refined Cell	Δ/%	Initial Cell	Refined Cell	Δ/%
a /Å	11.820	11.834	0.051	10.906	11.103	0.022	13.943	13.891	0.002
b /Å	6.222	6.142	0.010	6.923	6.855	0.007	7.542	7.536	0.007
c /Å	22.331	22.642	0.186	13.632	13.501	0.016	21.887	21.887	0.000
α /°	90.0	—	—	84.623	83.897	0.301	90.0	—	—
β /°	126.662	126.862	0.487	67.359	67.162	0.336	126.883	126.917	0.000
γ /°	90.0	—	—	76.404	75.878	0.133	90.0	—	—
Cell Type	Monoclinic			Triclinic			Monoclinic		
Volume /Å^3	1316.65			918.29			1831.93		

Thermal cure behaviors and processability

Differential scanning calorimetry (DSC) technique is the most commonly used method to investigate the thermal cure behaviors and processability of high-temperature polymers. In this work, the non-isothermal DSC curves of o-BDB, m-BDB and p-BDB monomers with ODA (~5 wt%) are shown in Fig. 3. The melting transitions occur at around 183.47, 183.58 and 251.52 °C, respectively, as displayed in Table 2. These differences in the melting point reflect that T_m has a strong relationship with the structure of monomers. Commonly, the melting point of para- monomer is higher than that of ortho- and meta- ones due to the symmetry and regularity of the monomers. The result can be interpreted by that the conformation of para groups is almost unchanged after rotated 180 ° around the main chain and melting entropy (ΔS) is low, leading to higher melting point.

Curing peaks are observed at 246.27, 253.67, and 256.97 °C for o-BDB monomer, m-BDB monomer and p-BDB monomer, respectively. In addition, it is noticeable that the curing peak temperature gradually rises along with the variation of the ortho-, meta- and para- position, indicating that ortho- monomer is most reactive among three monomers. It could be explained that ortho- monomer has more -CN density due to the close distance between pairs of nitrile, which is beneficial to contact the amino group to start the cure reaction.

View Article Online
DOI: 10.1039/C5RA15321B

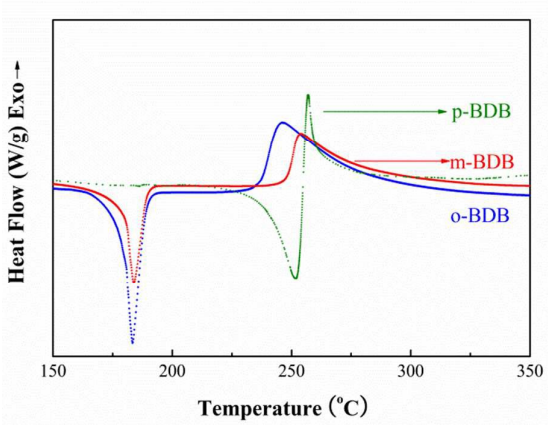

Fig. 3 DSC curves of o-BDB, m-BDB and p-BDB monomers with ODA (~5 wt%)

Table 2 DSC parameters of o-BDB, m-BDB and p-BDB monomers

Sample	Melting temperature /°C	Crosslinking temperature /°C	Processing windows /°C
o-BDB	183.47	246.27	62.80
m-BDB	183.58	253.67	70.09
p-BDB	251.52	256.97	5.45

It is also found that the monomers show different processing windows between melting point and curing temperature. Large processing windows make them suitable candidates for resin transfers and infusions in the molding process, etc. It is noted that m-BDB monomer has the broadest processing window (~70 °C) while p-BDB monomer has the narrowest window (~5 °C). Moreover, according to the processing degree, the broader the processing windows are, the easier the processing operations will be. Therefore, o-BDB and m-BDB monomers have more flexible processability than p-BDB monomer.

Structures of o-BDB, m-BDB and p-BDB polymers

O-BDB, m-BDB and p-BDB polymers are obtained via the prepolymerization and the postcure with ODA (~5 wt%) as a catalyst. FTIR and XRD techniques were used to characterize the structure of o-BDB, m-BDB and p-BDB polymers.

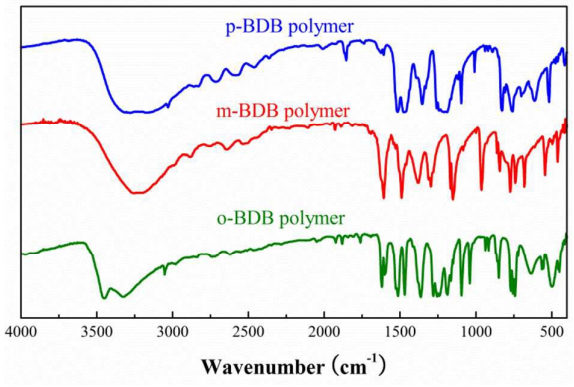

Fig. 4 FTIR spectra of o-BDB, m-BDB and p-BDB polymers

FTIR spectra of o-BDB, m-BDB and p-BDB polymers are compared in Fig. 4. As seen, the intensity of nitrile groups at 2230 cm^{-1} nearly disappears in the polymers because nitrile groups have been polymerized. It has been reported that the monomers are polymerized into triazine ring and phthalocyanine ring according to the appearances of triazine characteristic absorption at 1492 and 1370 cm^{-1} and phthalocyanine characteristic absorption at 1007 and 966 cm^{-1}, respectively. It is noticed that the appearance of the absorption peak at 1614 cm^{-1} appears, which is a characteristic stretching of amide groups (ODA). However, the peak intensity from p-BDB polymers is significantly weaker than those from o-BDB and m-BDB polymers. This is due to the higher melting temperature and curing temperature of p-BDB monomer compared to the other monomers, as explained earlier, which lead the volatilization of ODA and the decrease of amide groups in p-BDB polymer.

XRD patterns of o-BDB, m-BDB and p-BDB polymers are compared in Fig. 5. As seen, o-BDB, m-BDB and p-BDB polymers exhibit three non-crystalline diffraction humps centered at 22.9 °, 22.5 ° and 20.3 °, respectively. Those non-crystalline XRD peaks denote the frequent occurrence of particular interatomic distance (R) of a polymer in a largely disordered substance, and could be determined by Eq(1), as follows.

$$R = \frac{5}{4} \times \frac{\lambda}{2 \sin\theta} = 1.25\, d_{Bragg} \quad (1)$$

Where λ is the wavelength of X-ray and 2ϑ is the diffraction angle. The meaning of this expression is that the interatomic distance (R), a strong maximum in the diffraction pattern at angle ϑ, is equal to well-known Bragg equation. This equation is used to assess the most intense diffraction for non-crystalline materials. Consequently, interatomic distances of o-BDB, m-BDB and p-BDB polymers are determined to be 0.485, 0.494 and 0.546, respectively. The closer interatomic distances indicate that thermal stabilities and mechanical properties of o-BDB and m-BDB polymers would be more outstanding than p-BDB polymers after the postcuring process.

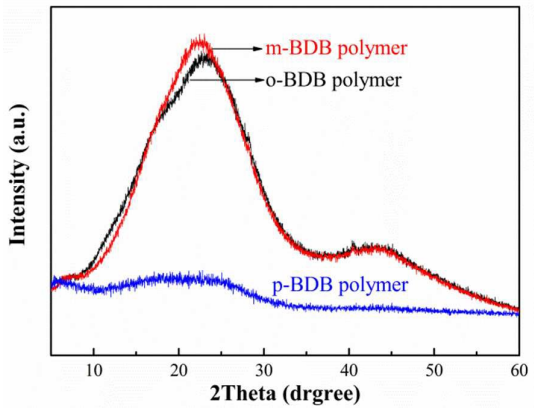

Fig. 5 XRD patterns of o-BDB, m-BDB and p-BDB polymers

Thermal stability

Thermal and thermal-oxidative stability of o-BDB, m-BDB and p-BDB polymers are evaluated by TGA, as shown in Fig. 6, and thermal parameters are collected in Table 3. The results indicate that all the three cured polymers show high temperatures of 5 %, 10 % and 50 % weight loss, not only in nitrogen but also in air, which reveals high thermal and thermal-oxidative stability. In addition, it is noteworthy that the char yields of cured polymers at 1000 °C are high over 57 %

View Article Online
DOI: 10.1039/C5RA15321B

in N_2, which indicates that these polymers can be used as high-temperature ablation materials probably. The high-temperature stability of these polymers is resourced from the cross-linked polymer network. Moreover, a low level of active H atoms on molecular structure ensures excellent oxidation stability due to the easy oxidation of active H atoms. However, m-BDB polymer exhibits higher weight loss temperature and char yield in N_2/air than o-BDB and p-BDB polymers. This indicates that thermal stabilities of these polymers are influenced by monomer structures, and m-BDB polymer is comparatively more stable towards the heat due to the higher curing temperature and crosslinking density.

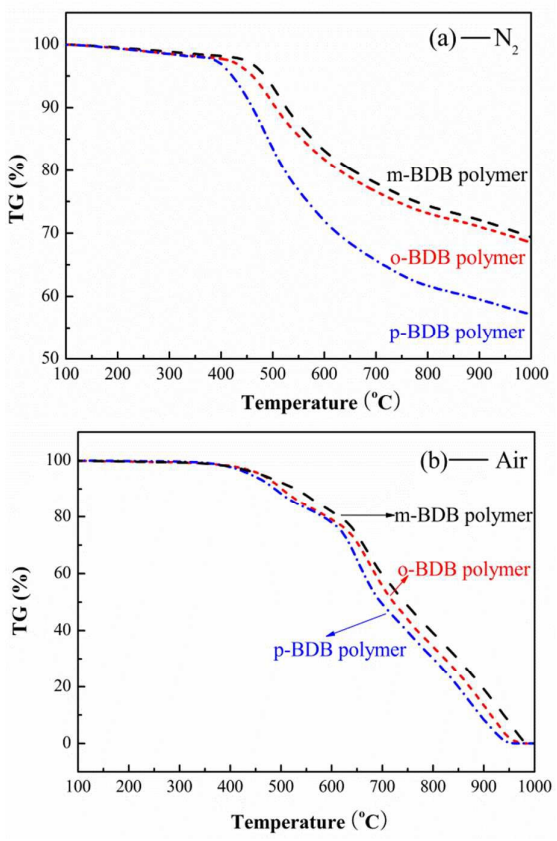

Fig. 6 TG plots of o-BDB, m-BDB and p-BDB polymers under N2 (a) and air (b) atmospheres

Dynamic mechanical properties

Dynamic mechanical behavior of o-BDB, m-BDB and p-BDB polymers in terms of storage modulus (E') and loss tangent (tan δ) are presented in Fig. 7. It can be found that storage moduli are 3716, 3362 and 1994 MPa at 25 °C for o-BDB, m-BDB and p-BDB polymers respectively, as shown in Fig. 7 (a). The storage moduli decrease with the increase of temperature gradually due to stress relaxation of the polymer network. The high storage moduli s observed for o-BDB and m-BDB polymers remain almost flat with the increase of temperature, which is believed to be due to the higher crosslinking density. However, there is a steady decrease in storage modulus observed for p-BDB polymer, indicating a lower overall crosslinking density, due to the volatilization of ODA in higher melting temperature. The loss tangent (tan δ) is the ratio of loss modulus to storage modulus, and the peak of tan δ curve is identified as glass transition temperature (T_g), which is vital for high-temperature polymers as it determines the upper limit of the application temperature. As seen in Fig. 7 (b), T_g of o-BDB, m-BDB and p-BDB polymers are 380, 384 and > 400 °C, respectively. DMA results reveal that monomer structures and curing temperatures are significantly important to influence the curing degree of phthalonitrile polymers, thus o-BDB and m-BDB polymers show higher mechanical properties than p-BDB polymers.

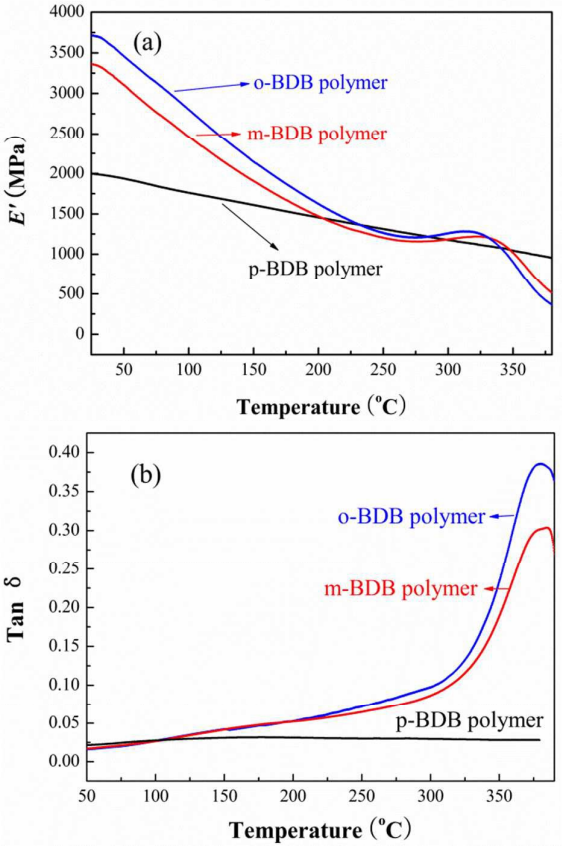

Fig. 7 DMA plots of o-BDB, m-BDB and p-BDB polymers versus temperature (heating rate = 10 °C min^{-1})

Table 3 Thermal parameters of o-BDB, m-BDB and p-BDB polymers

Sample	$Td_{5\%}$ / °C		$Td_{10\%}$ / °C		$Td_{50\%}$ / °C		Char yield at 1000 °C / %	
	In N_2	In air	In N_2	In air	In N_2	In air	In N_2	In air
o-BDB Polymer	460.8	461.6	506.2	501.8	>1000	721.3	68.5	0
m-BDB Polymer	485.0	462.0	526.1	528.3	>1000	743.8	69.4	0
p-BDB Polymer	421. 8	441.3	460.1	487.7	>1000	696.7	57.1	0

View Article Online
DOI: 10.1039/C5RA15321B

Journal Name

ARTICLE

Conclusions

A series of phthalonitrile monomers with o, m, p-dihydroxybenzene isomers were synthesized by a nucleophilic displacement reaction. The XRD results show that the unit cells of the o-, m-, p- monomers are monoclinic, triclinic and monoclinic, respectively. The melting temperatures of o-BDB and m-BDB polymers are around 183 ^{o}C, lower than p-BDB polymers by 68 ^{o}C. Curing behaviors of three monomers with 4,4′-diaminodiphenyl ether indicate that o-BDB and m-BDB monomers have lower curing temperatures and broader processing windows compared with the p-BDB monomer. Thermal and dynamic mechanical analyses reveal that o-BDB and m-BDB polymers exhibit more excellent thermal and thermal-oxidative stability and mechanical property than p-BDB polymers. All the three polymers have a high glass-transition temperature (> 380 ^{o}C). Therefore, based on excellent processability, superior thermal stability and outstanding mechanical property, o-BDB and m-BDB polymers are good candidates as high-temperature phthalonitrile polymers for applications such as structural components, high-temperature adhesives and packing materials in aerospace and microelectronic industries.

Acknowledgements

This work was supported by Program for Changjiang Scholars and Innovative Research Team in University (IRT13060) and Natural Science Foundation of Hebei Province, China (E2014202033).

References

1 M.J. Sumner, M. Sankarapandian, J.E. McGrath, J.S. Riffle and U. Sorathia, *Polymer*, 2002, **43**, 5069-5076.
2 A. Badshah, M. R. Kessler, Z. Heng, J. H. Zaidi, S. Hameed and A. Hasan, *Polym. Chem.*, 2013, **4**, 3617.
3 B. Amir, H. Zhou, F. Liu and H. Aurangzeb, *J. Polym. Sci. Pol. Chem.*, 2010, **48**, 5916-5920.
4 C. Hamciuc, I.-D. Carja, E. Hamciuc, T. Vlad-Bubulac and M. Ignat, *Polym. Advan. Technol.*, 2013, **24**, 258-265.
5 H.T. Sheng, X.G. Peng, H. Guo, X.Y. Yu, K. Naito, X.W. Qu and Q.X. Zhang, *Thermochim. Acta*, 2014, **577**, 17-24.
6 Z.B. Zhang, Z. Li, H. Zhou, X.K. Lin, T. Zhao, M.Y. Zhang and C.H. Xu, *J. Appl. Polym. Sci*, 2014, **131**, 20-27.
7 J.H. Hu, Y.C. Liu, Y. Jiao, S.C. Ji, R. Sun, P. Yuan, K. Zeng, X.M. Pu and G. Yang, *RSC Adv.*, 2015, **5**, 16199-16206.
8 S.B. Sastri, J.P. Armistead and T.M. Keller, *Polym. Composite*, 1996, **17**, 816-822.
9 S.B. Sastri, J.P. Armistead, T.M. Keller and U. Sorathia, *Polym. Composite*, 1997, **18**, 48-54.
10 D.D. Dominguez and T.M. Keller, *J. Appl. Polym. Sci.*, 2008, **110**, 2504-2515.
11 K. Jia, M. Xu, R. Zhao and X. Liu, *Polym. Int.*, 2011, **60**, 414-421.
12 H. Guo, Y. Zhan, Z. Chen, F. Meng, J. Wei and X. Liu, *J. Mater. Chem. A*, 2013, **1**, 2286-2296.
13 M.Z. Xu, J.Q. Hu, X.Q. Zou, M.D. Liu, S.H. Dong, Y.K. Zou and X.B. Liu , *J. Appl. Polym. Sci.*, 2013, **129**, 2629-2637.
14 M. Laskoski, D.D. Dominguez and T.M. Keller, *J. Polym. Sci. Pol. Chem.*, 2013, **51**, 4774-4778.
15 Z. Brunovska, R. Lyon and H. Ishida, *Thermochim. Acta*, 2000, **357**, 195-203.
16 G.P. Cao, W.J. Chen, J.J. Wei, W.T. Li and X.B. Liu, *Express Polym. Lett.*, 2007, **1**, 512-518.
17 R. Du, W. Li and X. Liu, *Polym. Degrad. Stabil.*, 2009, **94**, 2178-2183.
18 H.T. Sheng, X.G. Peng, H. Guo, X.Y. Yu, C.C. Tang, X.W. Qu and Q.X. Zhang, *Mater. Chem. Phys.*, 2013, **142**, 740-747.
19 T.M. Keller and D.D. Dominguez, *Polymer*, 2005, **46**, 4614-4618.
20 Y. Yang, Z. Min and L. Yi, *Polym. Bull.*, 2007, **59**, 185-194.
21 D. Augustine, D. Mathew and C. P. R. Nair, *Polym. Int.*, 2012, **62**, 1068-1076.
22 J.G. Young and W. Onyebuagu, *J. Org. Chem.*, 1990, **55**, 2155-2159.
23 S.B. Sastri and T. M. Keller, *J. Polym. Sci. Pol. Chem.*, 1999, **37**, 2105-2111.
24 F.H. Zhao, R.J. Liu, C. Kang, X.Y. Yu, K. Naito, X.W. Qu and Q.X. Zhang, *RSC Adv.*, 2014, **4**, 8383.
25 T.M. Keller, *J. Polym. Sci. Pol. Chem.*, 1988, **26**, 3199-3212.
26 X. Yang, Y. Lei, J. Zhong, R. Zhao and X. Liu, *J. Appl. Polym. Sci.*, 2011, **119**, 882-887.
27 A. Badshah, M.R. Kessler, Z. Heng and A. Hasan, *Polym. Int.*, 2014, **63**, 465-469.
28 D.D. Dominguez and T.M. Keller, *Polymer*, 2007, **48**, 91-97.
29 X.G. Peng, H.T. Sheng, H. Guo, K. Naito, X.Y. Yu, H.L. Ding, X.W. Qu and Q.X. Zhang, *High Perform. Polym.*, 2014, **26**, 837-845.